HUYGENS AEROTHERMAL ENVIRONMENT: RADIATIVE HEATING

E. Raynaud [(1)], Ph. Tran [(1)], J. Soler [(1)], M. Baillion [(1)]

[(1)]EADS SPACE Transportation, 66 route de Verneuil, 78133 Les Mureaux, France.
Email: elisabeth.raynaud@space.eads.net

ABSTRACT

Determination of the radiative heating fluxes was a crucial point in the sizing of Huygens's front heatshield. Radiative heating rates are mainly created in the shock-layer by highly non-equilibrium radiation of CN. The non-equilibrium model used by EADS-ST (formerly Aerospatiale) during the development phase of Huygens was challenged in 2004, due to new entry conditions. This paper presents the new EADS-ST collisional-radiative (CR) model, developed for Huygens pre-flight, in which non-equilibrium populations of excited states were calculated through a chemical kinetic scheme.

1. SCOPE OF THE PAPER

The successful entry of the Huygens probe in Titan's atmosphere on January 14th 2005 was allowed, among many things, by the correct sizing of the Thermal Protection System (TPS) covering the probe's front heatshield. The front heatshield was submitted to high heating rates, created by both convection and radiation in the shock layer.
EADS-ST (formerly Aerospatiale) was in charge of the development and sizing of the TPS, as well as of the estimation of the aerothermal environment imposed on the entering probe. Preliminary studies showed that radiative heating was important, and that the main contributor to radiation was CN, created at the shock from the dissociation of Titan's atmosphere two main components, N_2 and CH_4.
Due to the high speed and the low pressure at entry, the processes responsible for radiation are highly non-equilibrium. The sizing model used by Aerospatiale was thus a non-equilibrium model, based on the quasi-steady-state (QSS) assumption [1]. Recent updates on both the entry trajectories and the composition of the atmosphere rendered the development phase flux estimations obsolete and new estimations had to be obtained before the probe's release from the Cassini orbiter. The European Space Agency (ESA) gathered during the year 2004 an Aeroheating Convergence Working Group (ACWG), whose task was to review hypothesis, models, and deliver a safe estimation of the heating rates.
Within ACWG, the hypothesis of an equilibrium (Boltzmann) radiation calculation was retained, as a way to secure a maximal value of the radiative flux. However, this approach led to over-predicting fluxes that could not be endured by the TPS. In order to allow the flight of the probe and to refine the flux determination, EADS-ST proposed to rely on a revisited and more validated non-equilibrium approach.
The paper is organized as follows: in a first part, we present the thermochemical modelling of the shock and the plasma in the shock layer. The second part is a short description of the non-equilibrium radiation model used in the development phase. The third part describes the new collisional-radiative (CR) model as well as minor updates of the radiation modelling. Finally, we present our estimation of Huygens radiative heating, compared to various other calculations, and discuss the importance of various modelling.

2. AEROTHERMOCHEMICAL MODEL

Plasma modelisation of the shock layer surrounding the probe's heatshield is required for radiative flux computation. We use a decoupled approach : at first, a perfect gas, bidimensional inviscid flowfield is computed by an unsteady Euler code around the probe, in order to get the pressure field.
Using the Euler-calculated pressure field, and assuming conservation of enthalpy, we then calculate non-equilibrium chemistry, N_2 vibrational relaxation and electron temperature along the stagnation line.
For the Euler computations, the specific heat ratio γ is taken equal to 1.4 before the shock and to 1.3 in the shock layer. These values were obtained by comparison with 2D Navier-Stokes calculations. Temperatures at the shock are obtained by shock capturing, and the equivalent shock distance for radiative transfer calculations was evaluated at 11.5 cm.
The shock layer plasma is modelled as a perfect gas mixture of 20 species, reacting together according to 30 reactions. The chemistry used here is taken from [2] and [3]. Rotation is assumed to be in equilibrium with translation, and conservation equations are written for both vibrational and electron energy modes. Relaxation is calculated

with a Landau-Teller-type formula, with the Millikan & White model [4], with the two corrections of Park [5] for high temperatures (exchange rate and relaxation time). We use the Treanor & Marrone non-preferential model [6] to model the vibration - dissociation - vibration coupling (CVDV). The rate of exchange between translation and electron, and vibration and electron modes are calculated with the expressions of Candler [7]. The corresponding cross-sections were taken constant during the development phase, but in the current model (2004), they are functions of the free electron temperature, following [9]. Ionization reactions (controlling the production of reactions) are catalyzed by electrons, and by argon (for ionization of argon only). These aerothermal conditions were taken as the physical best estimate model in the reconstruction of shock tube experiments [19].

Fig. 1 shows the translational temperature, the vibrational temperature, and the free electron temperature obtained for a 77% N_2, 20% Ar, 3% CH_4 mixture, at a speed of 5046 m/s. The electronic temperature is lower than the vibrational temperature just after the shock, as the density of free electrons is low. However, as the electrons are the catalyst for the ionization reactions, a cascade happens as soon as a few electrons appear and the free electron temperature increases. Deeper in the shock layer, the N_2 vibrational coupling becomes the predominant process and the vibrational and free electron temperatures become alike.

Comparisons with LORE code, used by ESTEC teams within the ACWG group could be performed. The main differences between EADS-ST code and LORE are the following: LORE is a 3D code, which allows a more accurate determination of the shock position. However, the CVDV coupling was not used by ESTEC teams for Huygens (only vibration-dissociation coupling), nor the corrections of Park. The electronic energy relaxation was not modelled either. Further details on LORE utilisation for ACWG can be found in [21].

Fig. 2 shows the pressure and temperature comparison for the instant t=165 s in one of the Huygens entry 2004 trajectories (see below). Except near the shock region, a good agreement is found for the pressure and the translational temperature. However, the EADS-ST vibrational temperature is significantly lower than the LORE-computed one. The free electron temperature is very low (due to low ionization in this case) and goes strongly against the hypothesis T_v=T_e, often assumed when the electron energy equation is not computed.

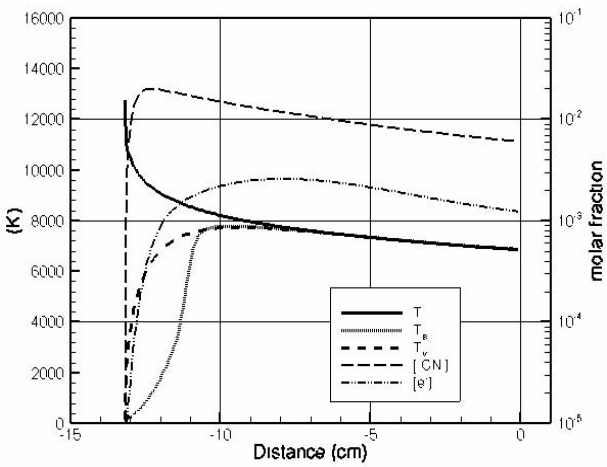

Fig. 1: Temperatures, CN and electron fractions in the shock laye, for a development phase trajectory and atmospheric composition.

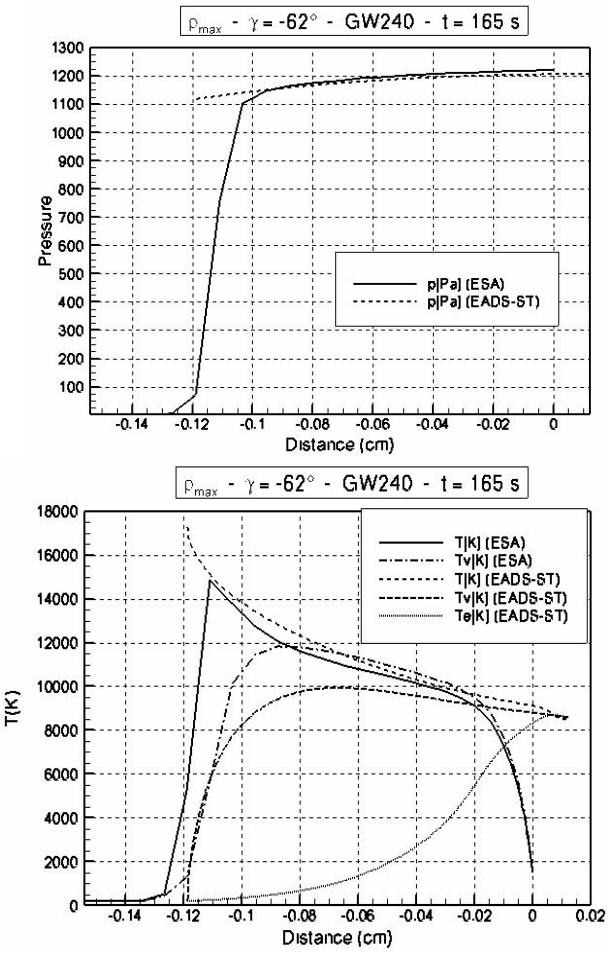

Fig. 2: Comparison of EADS-ST results with ESA/LORE calculations, with pressure (top panel) and the calculated temperatures (bottom panel). The free electron temperature is not calculated by LORE.

3. DEVELOPMENT PHASE MODEL FOR RADIATION

The radiation calculation was performed by Aerospatiale non-equilibrium radiation code, derived from NASA's NEQAIR 85. The populations of the electronic levels of CN were calculated through the QSS hypothesis [1]. The QSS model assumes that the rate of change of the density of each electronic level is much smaller than the population and depopulation rates, and can be neglected. The populating and depopulation mechanisms can be listed as the following:

- collisional excitation by electron-impact (EIC)
- collisional excitation by neutral-impact (NIC)
- collisional desexcitation by electron-impact
- collisional desexcitation by neutral-impact
- radiative desexcitation (RD)
- ionization by electron-impact (EII)
- ionization by neutral-impact (NII)
- recombination of ions by electron-impact (EIR)

In the case of a highly ionized flow, neutral-impact mechanisms can be neglected compared to electron-impact ones. For each electronic level *i* of each species, Eq. 1 is the traduction of the QSS hypothesis.

$$\sum_j K_{ij}^{EIC}.n_e N_j - N_i \times \sum_j K_{ji}^{EIC}.n_e - \sum_{j<i} A_{ij}^{RD} N_i + \sum_{j>i} A_{ji}^{RD} N_j + K_i^{EIR} N_+ n_e - K_i^{EII} N_i n_e = 0 \qquad (1)$$

In Eq. 1, N_i is the number density of level *i*, n_e the electron number density, and $\boldsymbol{A}_{ij}^{X}, \boldsymbol{K}_{ij}^{X}$ are respectively the radiative probability and the collision rate for process X occurring between states *i* and *j*. These reaction rates were calculated according to [1], from process-specific collisional cross sections.

Eq. 1, written for each level, forms a system of equations, whose variables are the number densities of electronically-excited states. This system is the master equation and can be completed by the species conservation equation.

In the case of Titan plasma, the neutral-impact processes were neglected during the development phase, but exchange reactions between vibrationally-excited N_2 and electronically -excited CN were found important. These reactions were taken into account, but due to the lack of knowledge, the reaction rates were assumed constant, without any dependence of the vibrational level of the colliding nitrogen molecule.

The resolution of the master equation leads to the population of the excited levels, from which radiation can be calculated. The original radiative module of the NEQAIR85 code (with amended electronic transitions moment functions for CN violet) was used for radiation calculation, and absorption was taken into account along the line of stagnation, in order to obtain the radiative flux at the wall on the stagnation point.

A thorough investigation of all sources of insufficient knowledge led to the estimation of 9 sources of uncertainties, such as the chemical model, the electron number density determination, other species radiation, or the methane mole fraction. Comparisons with different models of hypothesis yielded the associated margin, and allowed the proposal of a total margin of 75% on the calculated heating flux.

4. IMPROVEMENT OF THE PREFLIGHT CR MODEL

4.1 Why a new model?

The collisional-radiative (CR) model presented above was challenged within the ACWG, as non-experimentally validated and non-exhaustive. As a matter of fact, updates since Cassini's launch on the conditions of entry, and the composition of the atmosphere [18] led to a strong decrease in the predicted abundance of Argon, hence the computation of a much lower density of electrons. The influence of neutral-neutral collisional interaction, which had been neglected during the development phase, could justify the discard of the previous model.

In the first place, equilibrium calculations (with a Boltzmann distribution at T_v) were performed, but the resulting calculated heating flux on the TPS was too important. That is due to the fact that non-equilibrium populations of the excited electronic levels are much lower than the equilibrium ones as collisions do not equilibrate radiation.

In order to obtain a more realistic value, we re-visited our non-equilibrium model. The QSS hypothesis was retained, but doubts on the values of collisional cross sections led us to choose a different but more validated way to calculate the population and depopulation rates for excited species.

4.2 Pseudo-species reaction scheme

Collisional reactions rates can be calculated from the colliding partners cross sections and energies, as was done in the first QSS model (QSS92) [19], but they can also be calculated as chemical reaction rates, between the electronically excited molecules (such as CN $A^1\Pi$, $N_2A^3\Sigma$) as reacting species, with an Arrhenius-type formula :

Table 1: Set of reactions and parameters for the calculation of the forward rate

	Reaction	Parameters				Ref.
		τ (s)	A (cm^3/s/mole)	n	E (K)	
1	$CN + e^- \rightarrow CN_{(B)} + e^-$		6.24E+14 7.8E+13	0.5	37000.	[11]
2	$CN + e^- \rightarrow CN_{(A)} + e^-$		6.0E+14 6.0E+13	0.5	13300.	[11]
3	$CN + M \rightarrow CN_{(B)} + M$		1.8E+11 2.24E+10	0.5	37000.	[11]
4	$CN + M \rightarrow CN_{(A)} + M$		1.50E+11 1.50E+10	0.5	13300.	[11]
5	$CN_{(A)} \rightarrow CN_{(X)} + h\nu$	8.0E-06				[11]
6	$CN_{(B)} \rightarrow CN_{(X)} + h\nu$	6.25E-08				[11]
7	$N_{2(X)} + e^- \rightarrow N_{2(A)} + e^-$		2.40E+15	0.1	71610.	[15]
8	$N_{2(X)} + e^- \rightarrow N_{2(B)} + e^-$		2.75 E+16	-0.1	85740.	[15]
9	$N_{2(A)} + e^- \rightarrow N_{2(B)} + e^-$		2.68 E+15	0	13495.	[15]
10	$N_{2(X)} + M \rightarrow N_{2(A)} + M$		1.00E+12	-0.5	71610.	[15]
11	$N_{2(A)} + M \rightarrow N_{2(B)} + M$		1.2E+13	0.	13495.	[15]
12	$N_{2(C)} + M \rightarrow N_{2(X)} + M$		7.82E+12	0.	0.	[13]
13	$N_{2(A)} \rightarrow N_2 + h\nu$	2.0				[15]
14	$N_{2(B)} \rightarrow N_2 + h\nu$	7.0 E-06				[15]
15	$N_{2(C)} \rightarrow N_{2(B)} + h\nu$	4.2E-08				[13]
16	$CN_{(X)} + N_{2(v=4)} \rightarrow CN_{(A)} + N_2$		6.00E+13	0.	0.	[15]
17	$CN_{(X)} + N_{2(v=11)} \rightarrow CN_{(B)} + N_2$		6.00E+13	0.	0.	[15]
18	$CN_{(X)} + N_{2(A)} \rightarrow CN_{(B)} + N_{2(X)}$		7.2E+13	0.	0.	[14]
19	$C + N + N_2 \rightarrow CN_{(B)} + N_2$		5.7E-09	0.	0.	[14]
20	$N_{2(A)} + N_{2(A)} \rightarrow N_{2(B)} + N_{2(X)}$		4.63E+13	0.	0.	[14]
21	$N_{2(A)} + N_{2(A)} \rightarrow N_{2(C)} + N_{2(X)}$		9.03E+13	0.	0.	[14]

$$K = A \times T^n \times \exp\left(-\frac{E}{T}\right) \qquad (2)$$

The parameter E in Eq. 2 represents the activation energy of the reaction. Reactions between electronically-excited species have been studied for Mars [11, 12, 15] or Titan [14] atmospheric entries; the reactions rates were obtained experimentally and in some cases, theoretically validated.

We constructed a kinetic scheme for CN and N_2, in order to account for all collisional processes possible. Table 1 lists the reactions that were looked into in the scope of the model building.

The governing temperature in Eq. 2 is taken equal to the translational temperature T for neutral-impact collisions, and to the free electron temperature T_e for electron-impact collisions. For radiative desexcitation, the parameter τ is the life time of the excited state. Reactions 16 and 17 are the resonance reactions mentioned above, occurring between electronic levels of CN and vibrational levels of N_2. The excitation rate is calculated with Eq. 2, and the reacting population of $N_2(v)$ is calculated with a Boltzmann distribution for vibrational levels v=4 and v=11.

Reactions 20 and 21, although listed in Table 1, are not included till now in the model, as they lead to a non-linear system. Reaction 19 (inverse predissociation of the B state of CN) was discarded due to its negligible reaction rate. Backward reaction rates were calculated from the forward rates through the principle of detailed balance.

As can be seen in Table 1, 2 sets of parameters are available for the collisional excitation of CN, obtained experimentally by Russian institutes NiiMekh and Tsagi. Those sets could not be discriminated beforehand, and we built 2 kinetic schemes, one with the NiiMekh rates and the other with the Tsagi rates. The difference between the two schemes could provide an estimation of the uncertainty of the kinetic reaction rates.

In the following, we will call for convenience reactions 20 and 21 'pooling reactions', and reactions 16 and 17 'quenching reactions'. The

kinetic QSS model built for ACWG will be called QSS04, and the development phase model QSS92.

4.3 Non-equilibrium population calculations

Once the excitation and desexcitation rates are obtained with the previous kinetic data, the master equation is solved as before. Eq. 1 written for CN is amended with the addition of neutral-impact reaction rates (coming from reactions 3, 4, 17, 18, and 19).

Before continuing to the radiation calculations, we first examined the population calculations, in particular for the B state of CN, in order to determine the relative importance of each process. Fig. 3 shows the populations for the B state of CN, with the equilibrium model, the kinetic QSS model (QSS04), this same model but without pooling reactions, without quenching reactions, and finally (bottom panel) with each process (electron-impact, neutral-impact, and quenching) as unique contributor to excitation and desexcitation.

We can see in Fig. 3 that pooling reactions could totally be neglected, whereas quenching reactions should be taken into account, especially near the shock, where the electron density is still poor. Electron-impact processes are predominant from a distance of 10 cm from the wall, as the electron-density predicted by this aerothermal model becomes non negligible. Neutral-impact processes are as foreseen very important near the shock (due to the high translational temperature). We can also see that the B state population is much less important in a QSS model than in an equilibrium one. Such results show that except from pooling reactions, all processes play their part in the excitation and desexcitation mechanisms in the shock layer, and should be retained for a correct non-equilibrium modelling.

4.4 Updates of the radiative base

Comparisons of the spectral data were performed within ACWG, and only small discrepancies were found in comparison with the SPECAIR database [8]. However, in order to provide validated results and to ensure confidence in EADS-ST radiative results, the radiative database was up-dated from the compilation of C. Laux ([8]) since Huygens's flight. Beyond the scope of Huygens, this allowed EADS-ST to better the available radiative data for all air species, as far as line positions or transition probabilities for example are concerned. An example is proposed in Fig. 4, showing the spectrum of the $\Delta v=0$ band of $CN_{(B)}$, calculated with old data (QSS 04) or new data from [8]. The model related to the up-dated database is refered to by 'QSS05'.

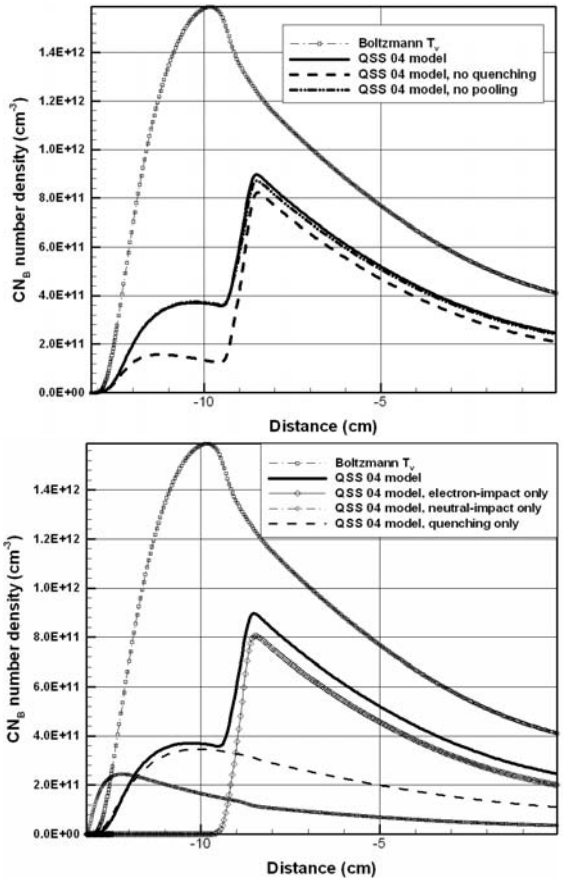

Fig. 3: Population of the B state of CN, in the shock layer. Top panel: equilibrium calculations, QSS04 full model, QSS04 without pooling, and QSS04 without quenching Bottom panel: equilibrium calculations, QSS04 full model and QSS04 with each of the important processes alone.

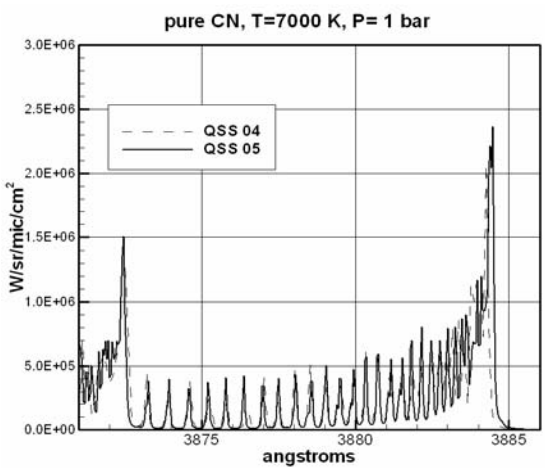

Fig. 4: $CN_{(B)}$ spectrum, before (QSS04) and after (QSS05) the up-date of the radiative database.

5. HUYGENS HEAT FLUX

5.1. Entry conditions

The atmospheric model of Yelle [18] gives three atmospheric profiles, compared in Table 2 to the Lellouch [17] maximal model. This last model prevailed during the development phase, because is maximized the radiative heating fluxes (due to the high abundance of argon). 3 trajectories were retained by Delta-Flight Acceptance Review, combining atmospheric composition and angle of entry: first the '-68° trajectory', i.e. minimal Yelle atmosphere, angle of entry -68°, gravity waves with phase 110 degrees, then the '-62° trajectory', i.e. maximal Yelle atmosphere, angle of entry -62°, gravity waves with phase 240 degrees, and finally the '-65° trajectory' i.e. nominal Yelle atmosphere, angle of entry -65°, no gravity waves. Calculations were made at first on the -62° trajectory, and then on the -65° one, which evolved to be the nominal trajectory for entry during ACWG work. For each of these trajectories, a few points spread along the time sequence were chosen for calculation in order to predict both accurate instantaneous heat flux and total heatload.

Table 2: Atmospheric models for Titan

	CH_4	Ar	N_2
Yelle Mini.	5%	0%	95%
Yelle Nom.	3%	2%	95%
Yelle Maxi.	1%	10%	89%
Lellouch	3%	21%	75%

5.2. Validation of the QSS hypothesis

The QSS hypothesis consists on neglecting the rate of change of each pseudo-species compared to all incoming and outgoing rates. The time taken by the system to reach the stationary density values is then shorter than the characteristic times of the involved processes. Without the QSS hypothesis, the densities N_i obey Eq. 3:

$$\frac{\partial N_i}{\partial t} = \sum_j K_{ij}^{EIC}.n_e N_j - N_i \times \sum_j K_{ji}^{EIC}.n_e + \sum_j K_{ij}^{EIC}.n_e N_j - N_i \times \sum_j K_{ji}^{EIC}.n - \sum_{j<i} A_{ij}^{RD} N_i + \sum_{j>i} A_{ji}^{RD} N_j + K_i^{EIR} N_+ n_e - K_i^{EII} N_i n_e \quad (3)$$

The calculation was made for the instant t=165s on the -62° trajectory. In Fig. 5, we show the time evolution of the population of $CN_{(B)}$, compared to the radiative lifetime, for 5 different points of the shock layer. We can see that the adjusting time is of the same order of magnitude that the radiative desexcitation time, which is the shortest caracteristic times of the processes listed in section 3. In the case of $CN_{(A)}$, the adjustment is much more rapid than the radiative desexcitation. We can conclude that the QSS hypothesis can be considered valid in the shock layer.

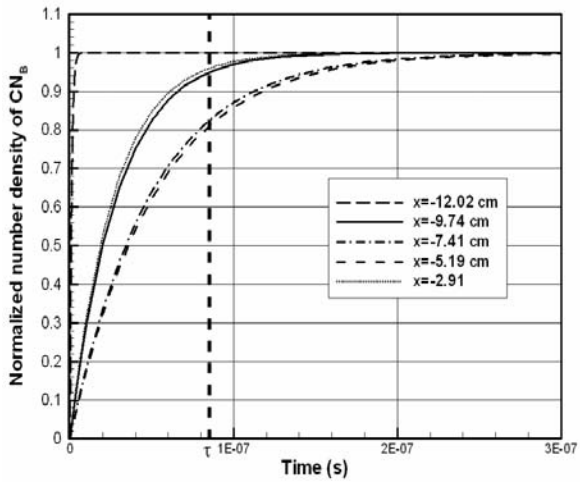

Fig. 5: Evolution of the number density of the B state of CN, at different points of the shock layer. The CN densities have been normalized to their equilibrium value for the comparison. The time τ is the radiative desexcitation time.

5.3 Kinetic CR vs equilibrium

The radiative heat fluxes for each trajectory are indicated in Fig. 6 and 7. Fig. 6 shows the different QSS models, for the -62° trajectory. The QSS 04 results, with both kinetic schemes, are compared with the challenged QSS 1992 ones (i.e. obtained with the development phase model). A hybrid model was also tested, in which electron-impact collisions are calculated by the former CR module, whereas neutral-impact collisions and quenching reactions are calculated with the 2004 kinetic QSS model. The equilibrium calculations are not shown in Fig. 6 for scale reasons, but the order of magnitude is at least 4 times the results of the different QSS models. In comparison to this large overestimation of the equilibrium results, all the QSS models show the same results. The 1992 results are hence reinforced ant the uncertainty due to the parameters of the kinetic reaction rates calculation is quite small.

In Fig. 7, we compare the different QSS models (QSS04 with both data sets, 04 hybrid, and QSS 92) to the equilibrium (i.e. Boltzmann distribution at T_v) calculations. The results obtained post-flight with the QSS05 model i.e. with the new radiative data ([8]) are shown as well. The QSS 92 results are presented with and without the +75% margin used for the TPS. As for the -62° trajectory, the recent QSS calculations, with the amended CR model, gives radiative heat fluxes well within the margin given during the development phase for the QSS 1992 calculations. Again, Boltzmann calculations are much too large in comparison, especially at high altitudes. The updating of the radiative database didn't change the result either, as we can see in Fig. 7.

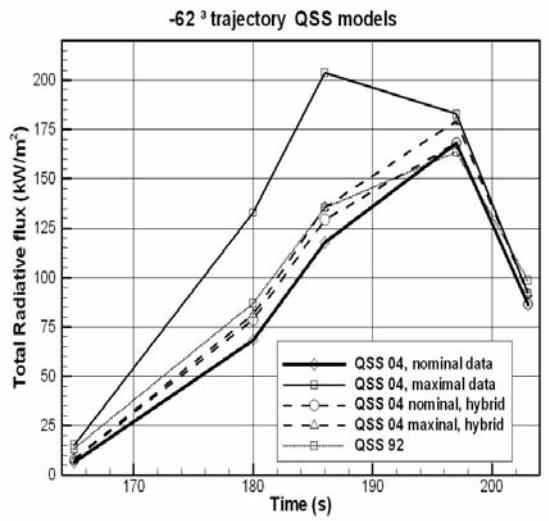

Fig. 6: QSS-calculated radiative heat fluxes for the -62° trajectory.

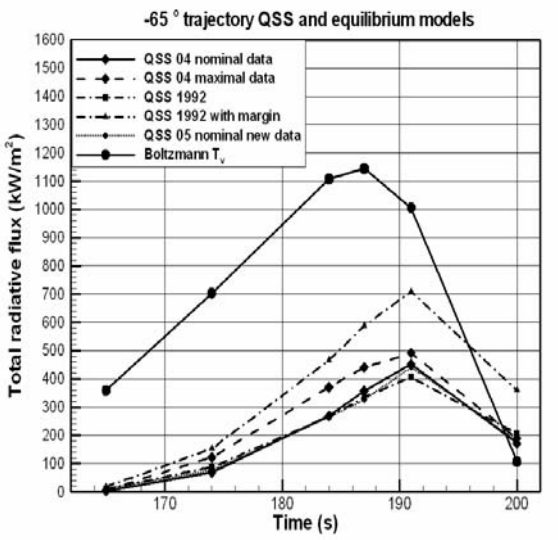

Fig. 7: Comparison of the various QSS calculations of the radiative heat flux with the equilibrium results, for the -65° trajectory.

5.4 Uncertainties modelling

In order to provide the results above with the corresponding margin, we conducted an uncertainty study similar to the one of the development phase [20].

First of all, as we are looking for a maximal value of the heating flux, the NiiMekh kinetic scheme was taken, as the most conservative data set. The uncertainties due to the calculation grid, neglected species radiation, shock stand-off distance determination or pressure level were retained from the 1992 determination [20]. Two sets of calculations were made for the nominal trajectory: one for which the electronic cross sections were taken not as constants but as polynoms [9] and the other in which the chemistry was altered and in particular the reaction of ionization of Argon. The results compared to the nominal model provide a margin due to the thermochemical modelling.

The obtained margin is shown in Fig. 8, where the EADS-ST 2004 results, with margin, are compared to the determination of other teams. All other ACWG teams' results are equilibrium calculations (ESTEC results with LORE-SPECAIR codes, and NASA with DPLR- NEQAIR 96 codes), with or without ions. NASA calculations were performed without taking on account absorption. The IPM results come from an independent non-equilibrium [16]. We present our equilibrium results (EADS-ST Boltzmann), and the QSS 2004 results, both with and without uncertainties.

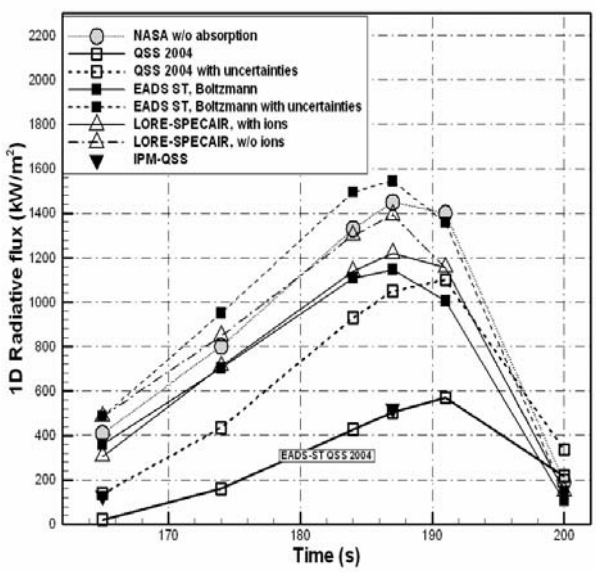

Fig. 8: Comparison of various teams results on the radiative heat flux for the nominal entry trajectory (see text)

We can see that all equilibrium calculations from ACWG teams predict the same level of flux. The apparent discrepancies come from the different hypothesis used to provide these calculations, i.e. the presence of ions, or taking into account absorption. However, all results fall within the margin predicted by EADS-ST Boltzmann results with uncertainties. The equilibrium results are much overpredicting in comparison to the EADS-ST non-equilibrium (QSS 2004) values, even when taking into account the modelized uncertainties. The independent results (IPM QSS) confirm our estimation of the non-equilibrium flux.

6. CONCLUSION AND PERSPECTIVES

Due to the need to obtain the closest estimate possible for the radiative heating flux on Huygens TPS, the non-equilibrium radiation model for air plasmas has been revisited and more validated than during the development phase. The collisional module of EADS-ST code has been increased with an alternative way to calculate excited-states population, i.e. with a kinetic scheme involving electronically-excited molecules as pseudo-species. An uncertainty study was also performed preflight in order to assess the confidence in the non-equilibrium approach in comparison to the over-predicting equilibrium one.
One main perspective is now essential to the planetary entry engineering community: going on with the improvement of industrial non-equilibrium radiation codes for air plasmas, in order to be able to better estimate both radiative and convective fluxes for the design of the TPS of the future entry vehicules.

7. REFERENCES

1. Park C., *Non equilibrium hypersonic aerothermodynamics*, Wiley, New York, 1989.
2. Park C. and Bershader D., Determination of the radiative emission of a hypersonic flow simulating the Cassini-Titan atmospheric entry probe environment, *AIAA* 90-1558.
3. Nelson H.F., Park C., and Whiting E.E., Titan atmospheric composition by hyper-velocity shock layer analysis, *J. Thermophys. Heat Tranfert*, 5, 2, 1991
4. Millikan R.C. and White D.R., Systematics of vibrational relaxation, *J.Chem.Physics,* 39, 12, 1963
5. Park C., Problems of rate chemistry in the flight regimes of aeroassisted orbital transfer vehicles, *AIAA* 84-1730, 1984
6. Marrone P.V. and Treanor C.E., Chemical Relaxation with preferential dissociation from excited vibrational levels, *The Physics of Fluids*, vol. 6, number 8, 1963.
7. Candler G. and Park C., The computation of radiation from non-equilibrium hypersonic flows, *AIAA* 88-2678.
8. Laux, C.O., *Optical Diagnostics and radiative emission of air plasmas*, Ph.D thesis, Stanford University, 1993.
9. William J., *Etude des processus physico-chimiques dans les écoulements détendus à haute enthalpie : application à la soufflerie à arc F4*, PhD thesis, Université de Provence, 1999.
10. Pancheshnyi S.V., Starikovskaia S.M., and Starikovski A.Y., Population of nitrogen molecule electron states and structure of the fast ionization wave*, J. Appl. Phys*., 32, 1999.
11. Kudryatsev N.N., Kuznetsova L.A. and Surzhikov S.T., Kinetics and nonequilibrium radiation of CO_2-N_2 waves, *AIAA* 2001-272.
12. Losev S.A., et al., Radiation of a mixture CO_2-N_2-Ar in shock waves : experiment and modelling, *Proc. 3rd European Symposium on Aerothermodynamics for Space Vehicles*, 1998.
13. Pancheshnyi S.V., Starikovskaia S.M., and Starikovski A. Y., Collisional deactivation of N_2 ($C^3\Pi$, v=0,1,2,3) states by N_2,O_2, H_2 and H_2O molecules*, Chem. Phys*., 262, 2000.
14. Pintassilgo C.D., Cernogora G., and Loureiro J., Spectroscopy study and modelling of an afterglow created by a low-pressure pulsed discharge in N_2-CH_4., *Plasma Sources Sci. Technol*, 10, 2001.
15. Chernyi G.G et al., Development of thermal protection systems for interplanetary fight, *Final Project Technical Report, ISTC* N03696, 1999.
16. Surzhikov S.T., private communication.
17. Lellouch E. and Hunten D.M., Titan atmosphere engineering model, *ESLAB* 87/199, 1987.
18. Yelle R.V., Strobel D.F, Lellouch E. and Gautier D., Engineering models for Titan atmosphere, *Proc. Huygens, Science, Payload and Mission*, 1997.
19. Baillion M., Taquin G. and Soler J., Huygens probe radiative environment, *Proc. 19th Intern. Symposium on shock waves*, 1993 .
20. Taquin G. et al., Huygens program Phases B2/B3, Aerothermodynamics studies, *HUY-AS/m-120-TN-0010 report*, 1992.

21. Walpot L., Caillault L., Molina R. and Laux C., Huygens entry heat flux prediction, *IPPW-3 Workshop,* 2005.